

Self-assembly and Li-ion storage performance of three new Nb/W mixed-addendum polyoxometalates based on the $\{\text{SiNb}_3\text{W}_9\text{O}_{40}\}$ clusters and transition-metal cations

Hai-Yang Wu,^{†a} Min Huang,^{†a} Chao Qin,^b Xin-Long Wang,^{*b} Hai Hu,^a Peng Huang,^{*a} and Zhong-Min Su^{*b}

^a Jiangsu Key Laboratory of Green Synthetic Chemistry for Functional Materials, Department of Chemistry, School of Chemistry and Material Science, Jiangsu Normal University, Xuzhou, 221116, PR China, E-mail: huangpeng@jsnu.edu.cn

^b Institute of Functional Material Chemistry, National & Local United Engineering Lab for Power Battery, Northeast Normal University, Changchun, 130024 Jilin, People's Republic of China. E-mail: wangxl824@nenu.edu.cn; zmsu@nenu.edu.cn.

1. Materials and Methods

All reagents were purchased from Aladdin Chemical Reagent Co., Ltd and were used as received without further purification. Precursors $\text{K}_7\text{H}[\text{Nb}_6\text{O}_{19}] \cdot 13\text{H}_2\text{O}$,¹ and $\text{Cs}_6\text{H}[\text{Si}(\text{NbO}_2)_3\text{W}_9\text{O}_{37}] \cdot 8\text{H}_2\text{O}$,² were synthesized according to the procedures described in the literature, and their purity was characterized by IR spectra, thermogravimetric analyses, and elemental analysis. Elemental analyses (Cs, Si, K, Mn, Co, Ni, W, and Nb) were determined with a Plasma-SPEC(I) ICP atomic emission spectrometer. IR spectra were recorded on Alpha Centaur FT/IR spectrophotometer (KBr pellets) over the region of 400–4000 cm^{-1} . PXRD patterns were recorded on a Siemens D5005 diffractometer with Cu $K\alpha$ ($\lambda = 1.5418 \text{ \AA}$) radiation in the range 3–50°. Thermogravimetric analyses (TGA) were performed on a Perkin-Elmer TGA 7 analyzer heated from room temperature to 800 °C under a nitrogen gas atmosphere with a heating rate of 10 °C min^{-1} (Fig. S6–S8).

2. Electrochemical Measurement

The working electrodes were prepared by compressing a mixture of active materials, acetylene black, and binder (polytetrafluoroethylene, PTFE) in a weight ratio of 70:20:10. The composite cathodes were cut into wafers with diameter of 8 mm with mass loading of 5 mg cm^{-2} . Lithium metal was used as the counter and reference electrode. The electrolyte was LiPF_6 (1.0 M) dissolved in a mixture of ethylene carbonate (EC), ethyl methyl carbonate (EMC) and dimethyl carbonate (DMC) with a volume ratio of 1:1:1. The LAND-CT2001A galvanostatic testers were employed to measure the electrochemical capacity at a current density of 100 mA g^{-1} and the cycle life of working electrodes at room temperature. The cutoff potentials for charge and discharge were set at 2.8 and 0.05 V (vs. Li^+/Li), respectively.

3. Synthesis

Synthesis of 1. The mixture of $\text{Cs}_6\text{H}[\text{Si}(\text{NbO}_2)_3\text{W}_9\text{O}_{37}] \cdot 8\text{H}_2\text{O}$ (60 mg) and MnCl_2 (15 mg) were put in a 5-cm high vial, which was then transferred and sealed in a Teflon-lined autoclave with 3 mL

HCl (aq. 1.0 M) and heated at 120 °C for 3 days followed by slow cooling to room temperature. The resulting products were blue block crystals (yield: 80%). Anal. Calc: Si, 0.88; Nb, 8.76; W, 52.03; Mn, 0.43; Cs, 9.40; K, 2.76. Found: Si, 0.73; Nb, 8.54; W, 52.91; Mn, 0.51; Cs, 8.99; K, 3.24. IR (KBr disks): 446, 533, 694, 780, 921, 962 cm⁻¹ (Fig. S3).

Synthesis of 2. Compound **2** was prepared following the procedure described for **1**, except for using CoCl₂ instead of MnCl₂. The resulting products were colorless block crystals (yield: 85%). Anal. Calc: Si, 0.88; Nb, 8.80; W, 52.25; Co, 0.46; Cs, 11.54; K, 1.23; Na, 0.54. Found: Si, 0.69; Nb, 9.42; W, 51.87; Co, 0.53; Cs, 10.76; K, 1.74, Na, 0.85. IR (KBr disks): 444, 527, 689, 778, 922, 966 cm⁻¹ (Fig. S4).

Synthesis of 3. Compound **3** was prepared following the procedure described for **1**, except for using NiCl₂·6H₂O instead of MnCl₂. The resulting products were colorless block crystals (yield: 83%). Anal. Calc: Si, 0.85; Nb, 8.45; W, 50.16; Ni, 0.44; Cs, 14.10; K, 1.18. Found: Si, 0.97; Nb, 9.08; W, 51.12; Ni, 0.66; Cs, 14.93; K, 1.57. IR (KBr disks): 420, 531, 692, 783, 923, 965 cm⁻¹ (Fig. S5).

4. Single-Crystal Studies

Intensity data of **1**, **2** and **3** were collected on a Bruker Apex CCD II area-detector diffractometer with graphite-monochromated Mo K α radiation ($\lambda = 0.71073 \text{ \AA}$) at 293 K. Absorption corrections were applied using multiscan techniques. Their structures were solved by direct methods of SHELXS-97 and refined by full-matrix least-squares techniques using the SHELXL-97 program.³ Anisotropic thermal parameters were used to refine all non-hydrogen atoms, with the exception of some oxygen atoms. Hydrogen atoms attached to lattice water molecules were not located. Crystallization water molecules were estimated by thermogravimetry, and only partial oxygen atoms of water molecules were achieved with the X-ray structure analysis. **1**: H₈₆Cs₉K₉MnSi₄Nb₁₂W₃₆O₁₉₉, $M_r = 12718.9$, Triclinic, $P-1$, $a = 12.960(5) \text{ \AA}$, $b = 19.166(5) \text{ \AA}$, $c = 20.622(5) \text{ \AA}$, $\alpha = 77.511(5)^\circ$, $\beta = 75.913(5)^\circ$, $\gamma = 83.394(5)^\circ$, $V = 4840(3) \text{ \AA}^3$, $Z = 1$, $\rho_{\text{calcd}} = 4.334 \text{ g cm}^{-3}$, final $R_1 = 0.0664$ and $wR_2 = 0.1906$ ($R_{\text{int}} = 0.0557$) for 17153 independent reflections ($I > 2\sigma(I)$). **2**: H₆₄Cs₁₁K₄Na₃CoSi₄Nb₁₂W₃₆O₁₈₈, $M_r = 12664.1$, Triclinic, $P-1$, $a = 12.999(5) \text{ \AA}$, $b = 19.174(5) \text{ \AA}$, $c = 20.681(5) \text{ \AA}$, $\alpha = 77.303(5)^\circ$, $\beta = 75.251(5)^\circ$, $\gamma = 83.327(5)^\circ$, $V = 4853(3) \text{ \AA}^3$, $Z = 1$, $\rho_{\text{calcd}} = 4.462 \text{ g cm}^{-3}$, final $R_1 = 0.0695$ and $wR_2 = 0.2085$ ($R_{\text{int}} = 0.0510$) for 23285 independent reflections ($I > 2\sigma(I)$). **3**: H₈₆Cs₁₄K₄NiSi₄Nb₁₂W₃₆O₁₉₉, $M_r = 13191.7$, Triclinic, $P-1$, $a = 13.010(5) \text{ \AA}$, $b = 19.204(5) \text{ \AA}$, $c = 20.756(5) \text{ \AA}$, $\alpha = 77.307(5)^\circ$, $\beta = 75.046(5)^\circ$, $\gamma = 83.226(5)^\circ$, $V = 4877(3) \text{ \AA}^3$, $Z = 1$, $\rho_{\text{calcd}} = 4.462 \text{ g cm}^{-3}$, final $R_1 = 0.0917$ and $wR_2 = 0.2897$ ($R_{\text{int}} = 0.0635$) for 17043 independent reflections ($I > 2\sigma(I)$).

CCDC 1841400 (**1**), 1841401 (**2**) and 1841402 (**3**) contain supplementary crystallographic data for this paper. These data can be obtained free of charge from the Cambridge Crystallographic Data Centre via www.ccdc.cam.ac.uk/data_request/cif for **1**, **2**, and **3**.

Table S1. The fitting errors of the simulated equivalent circuit of **1**, **2**, and **3** anodes.

| | Compound 1 | Error | Compound 2 | Error | Compound 3 | Error |
|-----|-------------------|--------|-------------------|--------|-------------------|--------|
| Re | 2.699 | 5.759 | 1.901 | 1.752 | 0.026 | 9.311 |
| Rf | 19.35 | 4.177 | 12.80 | 15.290 | 37.96 | 12.760 |
| Rct | 173.6 | 12.170 | 179.4 | 0.885 | 183.5 | 4.739 |

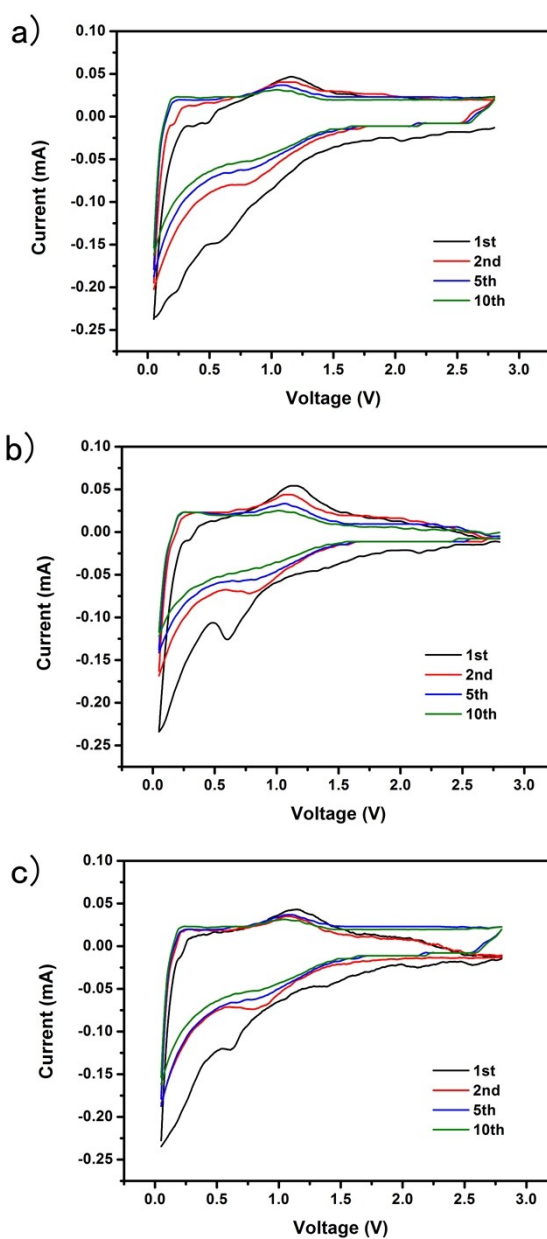


Fig. S1 CV profiles of **1**, **2**, and **3** at a scan rate of 0.1 mV s⁻¹.

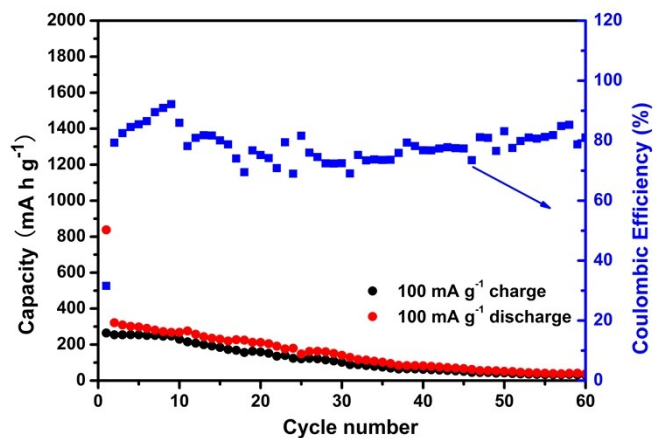


Fig. S2 Cycling performance of $\text{Cs}_6\text{H}[\text{Si}(\text{NbO}_2)_3\text{W}_9\text{O}_{37}] \cdot 8\text{H}_2\text{O}$ at a current density of 100 mA g^{-1} .

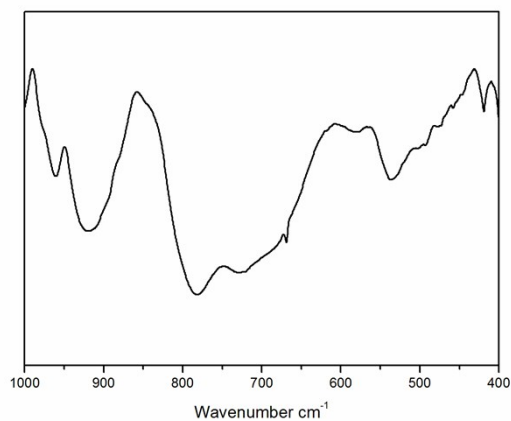


Fig. S3 The IR spectrum of **1**. IR (KBr disks): 446 and 533 cm^{-1} $\nu(\text{W-O-Si})$, 694 cm^{-1} $\nu(\text{Nb-O-Nb})$, 780 and 921 cm^{-1} $\nu(\text{W-O-W})$, 962 cm^{-1} $\nu(\text{W=O})$.

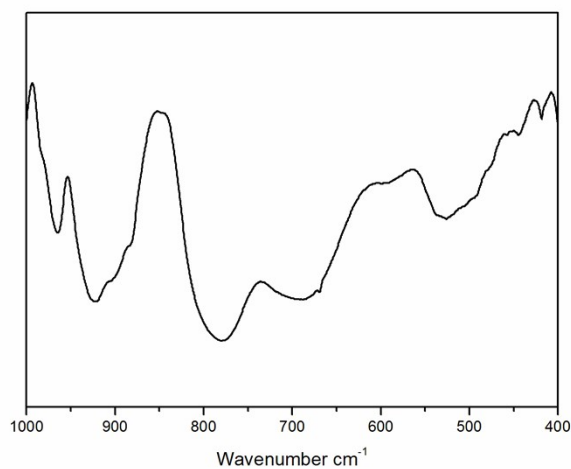


Fig. S4 The IR spectrum of **2**. IR (KBr disks): 444 and 527 cm^{-1} $\nu(\text{W-O-Si})$, 689 cm^{-1} $\nu(\text{Nb-O-Nb})$, 778 and 922 cm^{-1} $\nu(\text{W-O-W})$, 966 cm^{-1} $\nu(\text{W=O})$.

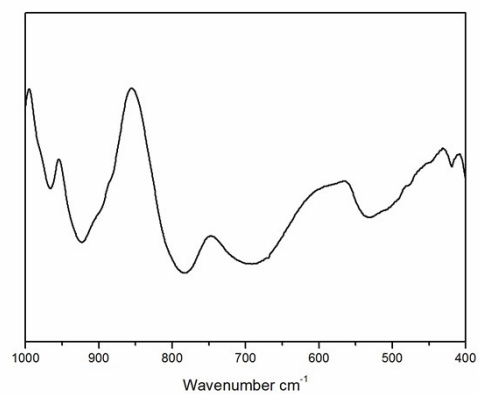


Fig. S5 The IR spectrum of **3**. IR (KBr disks): 420 and 531 cm^{-1} $\nu(\text{W-O-Si})$, 692 cm^{-1} $\nu(\text{Nb-O-Nb})$, 783 and 923 cm^{-1} $\nu(\text{W-O-W})$, 965 cm^{-1} $\nu(\text{W=O})$.

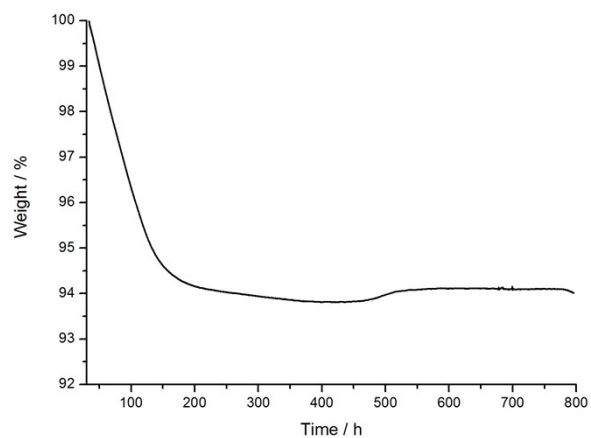


Fig. S6 The TGA curve of **1**.

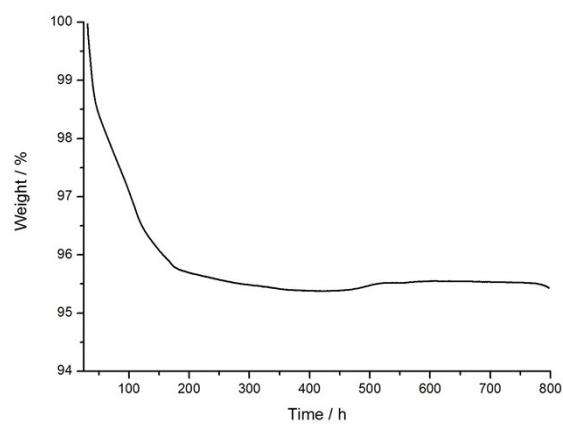


Fig. S7 The TGA curve of **2**.

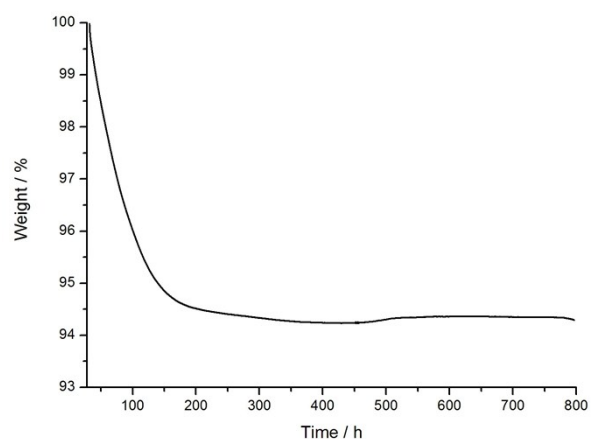


Fig. S8 The TGA curve of **3**.

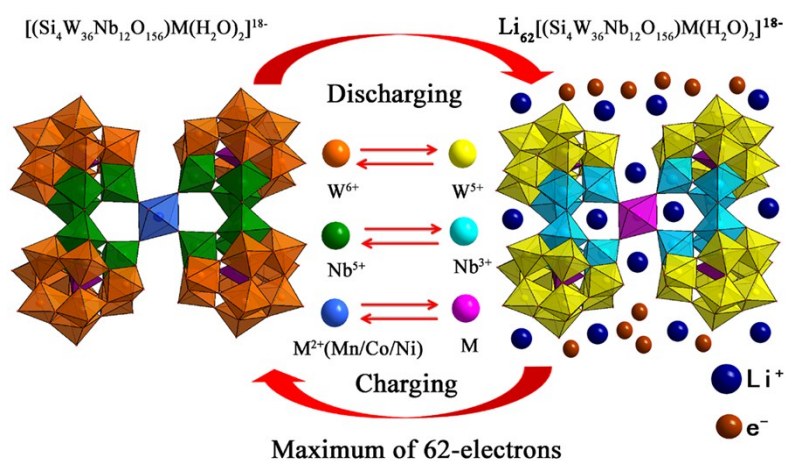
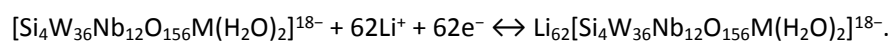


Fig. S9 Schematic diagrams of the possible mechanism for the capacity of **1**, **2** and **3**.

The battery behaviors of **1**, **2**, and **3** are achieved by redox of metal ions (W, Nb, Mn, Co and Ni) of the POMs. The W^{6+} and Nb^{5+} are usually reduced to W^{5+} and Nb^{3+} , respectively.^{4,5} Transition metal ions Mn^{2+} , Co^{2+} , and Ni^{2+} in the POMs are usually reduced to Mn, Co, and Ni, respectively.^{6, 7, 8} Based on this, a possible mechanism for the battery behavior of **1**, **2**, and **3** was proposed in **Fig. S9**. Maximum 62 Li ions per formula could be inserted into the material, and the overall equation of lithium ions insertion/extraction reaction can be expressed as follows:



References

- 1 M. Filowitz, R. K. C. Ho, W. G. Klemperer, W. Shum, *Inorg. Chem.*, 1979, **18**, 93.
- 2 G. S. Kim, H. Zeng, W. A. Neiwert, J. J. Cowan, D. VanDerveer, C. L. Hill and I. A. Weinstock, *Inorg. Chem.*, 2003, **42**, 5537.
- 3 G. M. Sheldrick, *SHELXL-97, Program for the Refinement of Crystal Structure*; University of

Göttingen: Germany, 1997.

4 W. Ye, H. Yu, X. Cheng, H. Zhu, R. Zheng, T. Liu, N. Long, M. Shui, J. Shu, *Electrochimica Acta* 2018, **292**, 331.

5 L. Yan, J. Shu, C. Li, X. Cheng, H. Zhu, H. Yu, C. Zhang, Y. Zheng, Y. Xie, Z. Guo, *Energy Storage Materials*, 2019, **16**, 535.

6 Y. Yue, Y. Li, Z. Bi, Gabriel M. Veith, Craig A. Bridges, B. Guo, J. Chen, David R. Mullins, Sumedh P. Surwade, S. M. Mahurin, H. Liu, M. Parans Paranthaman and S. Dai, *J. Mater. Chem. A*, 2015, **3**, 22989.

7 F. Shen, Y. Wang, S. Li, J. Liu, L. Dong, T. Wei, Y. Cui, X. L. Wu, Y. Xu and Ya. Lan, *J. Mater. Chem. A*, 2018, **6**, 1743.

8 S. Xia, F. Li, Xue Li, F. Cheng, C. Sun, J. Liu and H. Guo, *Dalton Trans.*, 2018, **47**, 5166.